Available online at www.sciencedirect.com
SCIENCE DIRECT
Polymer 46 (2005) 3639–3648
polymer
www.elsevier.com/locate/polymer

Silylation of hyaluronan to improve hydrophobicity and reactivity for improved processing and derivatization

Min Zhang[1], Susan P. James*

Department of Mechanical Engineering, Biomedical Engineering Program, Colorado State University, Fort Collins, CO 80523-1374, USA

Received 6 October 2004; received in revised form 22 February 2005; accepted 7 March 2005
Available online 31 March 2005

Abstract

A novel hyaluronan (HA) derivative was synthesized through silylation reaction to improve the hydrophobicity of HA, to enhance its solubility in common organic solvents, and to make it more reactive for further derivatizations (e.g. esterification). While HA can not be silylated directly, its ion-paired complex with a long aliphatic chain quaternary ammonium salt (HA–CTA) was an effective starting material for the silylation reaction. The degree of silylation (DS) was controlled by changing the reaction parameters such as temperature, time and amount of silylation reagent. Silylated HA–CTA with a high DS (>3.2) was soluble in xylenes and hexane, while that with a low DS ($3.2>DS>2.5$) was only soluble in acetone, THF and 1,2-dichloroethane. The silyl groups and ammonium cations were also easily removed through hydrolysis to regenerate the native HA.

Keywords: Hyaluronan; Silylation; Polysaccharides

1. Introduction

Hyaluronan (HA) is a naturally occurring polysaccharide, present in all vertebrate tissues and body fluids [1]. Due to a unique set of physical and biological properties, such as viscoelasticity [1], hydrophilicity [2–4], lubricity [4,5] and cell-activity regulation [6], HA has been established as one of the most effective biopolymers. Its applications include viscosupplementation in arthritic therapy [7]; tissue separation and protection in ophthalmic, abdominal, orthopedic and other viscosurgeries; postoperative adhesion prevention [8–10]; drug delivery devices [11]; tissue engineering scaffolds [12]; wound repair devices [13]; and biocompatible and lubricious coatings [14].

However, its extreme hydrophilicity and quick turn-over [15] in the body environment limit the application of HA for permanent implants, and its use in conjunction with durable, hydrophobic biomaterials, such as ultra high molecular weight polyethylene (UHMWPE) used in total joint replacements. The objective of this study was to modify HA to improve its hydrophobicity, solubility in common organic solvents, compatibility with other more hydrophobic biomaterials, and reactivity for further derivatization.

Silylation has long been recognized as an effective method to prepare organic-soluble derivatives of polysaccharides and improve hydrophobicity [16] by replacing the active hydrogen in polysaccharides with trimethylsilyl ($-Si(CH_3)_3$) groups [17]. Cellulose is the most reported polysaccharide that has been successfully silylated. In the paper and textile industry, cellulose was silylated to improve its solubility in organic solvents [16,18], or to produce a melt-processable derivative [19,20]. Various combinations of silylation reagents and solvents, such as trimethylchlorosilane (TMCS) in pyridine [21], N,O-bis(trimethylsilyl)acetamide (BSA) in dimethylsulfoxide (DMSO) [22] and hexamethyldisilazane (HMDS) in liquid ammonia [18], have been successfully used to obtain trimethylsilylcelluloses. Compared with cellulose, chitin is more difficult to silylate [16], but β-chitin was completely silylated with a mixture of HMDS and TMCS in pyridine at 70 °C [23]. A series of silyl dextrans soluble in a variety of organic solvents were also obtained with HMDS in DMSO [24].

* Corresponding author. Tel.: +1 970 4912842; fax: +1 970 4913827.
E-mail address: susan.james@colostate.edu (S.P. James).
[1] Present address: Department of Bioengineering, University of Washington, Mail Box 351750, Seattle, WA 98195, USA.

0032-3861/$ - see front matter © 2005 Elsevier Ltd. All rights reserved.
doi:10.1016/j.polymer.2005.03.022

Although HA is similar in some degree to cellulose, chitin and dextran in structure, it cannot be silylated with the same methods, and there are no reports in the literature regarding silylation of HA. Silylation of HA is particularly difficult because of strong hydrogen bonding within and among molecules and its insolubility in any of the common silylation solvents. Scott [25,26] found that long paraffin-chain quaternary ammonium compounds, such as cetyltrimethylammonium bromide (CTAB), could be used to precipitate polyanions of hyaluronan and various sulfuric polysaccharides from aqueous solution as polysaccharide–ammonium salt complexes, and that these complexes were soluble in salt solutions (e.g. NaCl) and in some highly polar organic solvents. Therefore, the complexes of HA with aliphatic quaternary ammonium cations soluble in highly polar organic solvents can be used as intermediates for further modifications.

In this investigation, an effective method to silylate HA was developed. With a complex between HA and the long aliphatic chain ammonium cation as the starting material, HA was successfully silylated, and the silyl derivative could be regenerated via hydrolysis. The effect of the silylation process on the molecular weight of HA was investigated to determine whether the reaction conditions caused chain scission. The thermal properties were also investigated because use of silylated HA in further processes, such as forming a composite with a hydrophobic polymer, required knowledge of the thermal properties.

2. Experimental

2.1. Materials

Sodium hyaluronate (HyluMed®, medical grade, molecular weight: 1.36×10^6 Da) was purchased from Genzyme (Cambridge, MA) and stored at 2–8 °C. Cetyltrimethylammonium bromide (CTAB), hexamethyldisilazane (HMDS, 99.9%), trimethylchlorosilane (TMCS, redistilled, 99+%, contains <0.1% dimethyldichlorosilane), and *N*,*O*-bis(trimethylsilyl)acetamide (BSA) were obtained from Aldrich (Milwaukee, WI). HMDS, TMCS and BSA were stored at 4 °C. Silylation grade dimethylsulfoxide (DMSO) was purchased from Pierce (Rockford, IL). Xylenes, dimethylformamide (DMF), pyridine and tetrahydrofuran (THF) were purchased from Fisher (Pittsburgh, PA), and were respectively dried by refluxing over Na, CaH_2, CaO and Na, and distilled just before use. All other common solvents used in this study were also purchased from Fisher, except ethanol (ACS/USP grade), which was purchased from Pharmco (Brookfield, CT). Deuterium oxide (D_2O, D 99.9%), chloroform-*d* ($CDCl_3$, D 99.8%) and dimethyl sulfoxide-d_6 (D 99.9%) were purchased from Cambridge Isotope Laboratories, Inc. (Andover, MA). All chemicals were used as received unless specified.

2.2. Reactions

2.2.1. Precipitation of HA with ammonium salt

Sodium hyaluronate (1.5 g) was dissolved in 600 ml of distilled water. CTAB (1.5 g) was dissolved in 300 ml of distilled water. The CTAB solution was slowly added to the HA solution with magnetic stirring. With the addition of CTAB, the solution mixture became more and more opaque. When close to the reaction end point, several more drops of CTAB made HA coagulate completely, while the supernatant became a clear solution. The white precipitate (HA–CTA) was centrifuged, washed with distilled water several times to remove CTAB residue, and then dried in a vacuum oven at 50 °C for at least 24 h.

2.2.2. Silylation of HA-ammonium complex

The above dry precipitate (HA–CTA) was cut into small pieces and charged into a 250 ml 3-neck flask, and then 50 ml of DMSO were added under dry N_2. The mixture was left overnight for swelling of HA–CTA, and then heated at 60 °C for about 4 h. Once all the HA–CTA particles had dissolved, 25 ml of HMDS were added to the above solution. The silylation reaction was carried out at 55–75 °C for a desired period of time, with stirring and under N_2 flow. In the resulting two-phases of light yellow solution, the upper HMDS layer contained silylated HA–CTA, which was separated from the bottom DMSO layer, dried under vacuum (pressure: ~25 in. Hg vacuum) in 50 °C water bath to remove HMDS, and then washed with xylenes five times, yielding light yellow silyl HA–CTA powder.

2.2.3. Regeneration of HA from HA–CTA

HA–CTA (200 mg) was dissolved in 10 ml of 0.2 M NaCl solution. HA was precipitated from the solution with 2–3 volumes of ethanol. The precipitate was then washed with ethanol several times to remove –CTA residue. To remove NaCl residue, the regenerated HA was dissolved in distilled water and re-precipitated with 2–3 volumes of acetone. The resulting precipitate was collected and vacuumed at 50 °C for 24 h. The anhydrous, regenerated HA was a white bulk material.

2.2.4. Regeneration of HA from silyl HA–CTA

Silyl HA–CTA (200 mg) was dissolved in the mixture of 0.4 M NaCl aqueous solution (5 ml) and ethanol (5 ml). HA was precipitated with 1–2 volumes of ethanol. The precipitate was washed with ethanol several times to remove –CTA residue and hexamethyldisiloxane (a byproduct from the reaction between $-Si(CH_3)_3$ and water). The NaCl residue was removed with the same method described above for HA regeneration from HA–CTA.

2.3. Characterization methods

2.3.1. Fourier transform infrared spectroscopy (FT-IR)

A Nicolet Magna-IR 760 spectrometer (E.S.P.) (Nicolet

Instrument Corporation, WI) was used to record FT-IR spectra. The sample powder was ground and mixed with KBr (1%, w/w), and then pressed into pellets for analysis. Transmission absorption spectra were collected over a range of 600–4000 cm^{-1} at a resolution of 4 cm^{-1} with 128 scans.

2.3.2. X-ray photoelectron spectroscopy (XPS)

XPS analyses were performed on a PHI 5800 spectrometer (Physical Electronics, Inc., MN). The instrument was equipped with a monochromatic Al K_α (1486.6 eV) X-ray source. A low energy (5 eV) electron gun was used for charge neutralization on the non-conducting samples. Measurements were taken with an electron takeoff angle of 45 ° from the surface normal (sampling depth ~50 Å). Surface elemental compositions were determined from 0 to 1000 eV survey scans acquired with a pass energy of 100 eV. High resolution N1s spectra were obtained at a pass energy of 25 eV. Component peak analysis of high resolution spectra was performed using XPSPeak 4.1 software. HA, HA–CTA and silyl HA–CTA samples were respectively dissolved in water, DMSO and xylenes, and then cast into films for analysis.

2.3.3. Nuclear magnetic resonance (NMR)

^1H and ^{13}C NMR spectra were recorded using a Varian Inova 300 NMR spectrometer (Varian, Inc , CA) operating at 300 MHz. The number of scans for ^1H spectra was 32, while for ^{13}C spectra, the scan was continued until a satisfactory spectrum was obtained. HA, HA–CTA and silyl HA–CTA analysis samples were prepared respectively in deuterium oxide, dimethyl sulfoxide-d_6 and chloroform-*d*. The concentration for ^1H spectra was approximately 25 mg/ml, while that for ^{13}C was approximately 50 mg/ml.

2.3.4. Silicon elemental analysis

Silicon (Si) elemental analysis was performed at Galbraith Laboratories (Knoxville, TN). The silicon content was determined using inductively coupled plasma optical emission spectroscopy (ICP-OES), after peroxide fusion in a Parr bomb.

2.3.5. Determination of the degree of silylation (DS)

The DS was determined using three methods: weight gain (Δw), Si content (%Si), and FT-IR. The DS calculation formula from Δw and %Si were derived from those used for silyl cellulose [21,27].

DS from weight gain:

$$\mathrm{DS} = \frac{\Delta w \times 662.846}{w_0 \times 72.184}$$

DS from Si content:

$$\mathrm{DS} = \frac{\%\mathrm{Si} \times 662.846}{28.06 - \%\mathrm{Si} \times 72.184}$$

In the above two equations, 662.846 represents the molecular weight of the HA–CTA disaccharide unit, 72.184 is the change of group weight from –H to $-Si(CH_3)_3$, w_0 is the weight of original HA–CTA, and 28.06 is the atomic mass of Si.

For the FTIR method, the peak area (A) change of –OH groups was used to calculate the DS. In silylation, with the replacement of –OH by $-OSi(CH_3)_3$, the stretching vibration peak of –OH at approximately 3500 cm^{-1} (A_{3500}) decreases, and because this decrease is proportional to the degree of silylation it can be used for the determination of DS. The vibration bands of C–O in alcohols and C–O–C in glycoside overlap at 1046–1150 cm^{-1} [28]. These peaks do not change during silylation and can be used as the internal reference (A_{ref}) to calculate the DS.

$$\mathrm{DS} = 4 \times \frac{(A_{3500}/A_{\mathrm{ref}})_{\mathrm{HA-CTA}} - (A_{3500}/A_{\mathrm{ref}})_{\mathrm{silyl}}}{(A_{3500}/A_{\mathrm{ref}})_{\mathrm{HA-CTA}}}$$

2.3.6. Thermal degradation of HA

A 1.0 g/l HA solution in 0.2 M NaCl was prepared and filtered through Whatman No.50 paper. The solution was divided into several 50-ml aliquots, put in sterile plastic tubes and degraded in an oil bath set at the temperature of interest. At the end of the desired exposure intervals, the tubes were removed, immediately immersed in ice water for 5 min, and then stored in a refrigerator at 4–8 °C until molecular weight measurement [29].

The molecular weight (M_w) of HA was calculated based on viscosity measurement [30,31]. After degradation, the aliquots were diluted to concentrations of 0.8, 0.6, 0.4, and 0.2 g/l, respectively. The efflux time of 0.2 M NaCl solution (t_0) and the HA solutions (t) was determined by using an Ubbelohde capillary viscometer (size: 1C, Cannon Instrument Co., PA) in a 25 °C water bath. After equilibration at the test temperature for about 30 min, the flow times (t) of the solutions were measured and compared to pure solvent (t_0). Three observations were made for each sample and the averages were taken.

The relative viscosity of the HA solution is t/t_0, while the specific viscosity is $t/t_0 - 1$. By plotting (specific viscosity/HA concentration) vs. HA concentration, a straight line was obtained, and its y-intercept is the intrinsic viscosity [η] of HA. The relationship between [η] and M_w was described by the Mark–Houwink–Sakurada equation [32]:

$$[\alpha] = KM_w$$

K and α are the constants related with solvent, temperature and polymer. For HA solution tested in 0.2 M NaCl at 25 °C, the constants ($K = 0.0228$ ml/g, $\alpha = 0.816$) were provided by the HA manufacturer, Genzyme.

2.3.7. Thermal gravimetric analysis (TGA)

The thermal stability of HA and its derivatives were determined using a Seiko TG SCC 5200 thermal gravimetric analysis (TGA) at a heating rate of 10 °C/min in air. Prior to

each test, the temperature was equilibrated at the starting point for 5 min.

3. Results and discussion

3.1. Complex of HA with ammonium salt

The complex HA–CTA is actually a salt between hyaluronic acid and the ammonium base. The complexing reaction is shown in Fig. 1(a). The difference between the native HA and HA–CTA structures was confirmed with FT-IR, XPS and NMR analysis. In the FT-IR spectra shown in Fig. 2, absorption of hydrocarbon-associated bands in HA–CTA at 2926 and 2855 cm^{-1} increase markedly compared to HA. Introduction of a large amount of $–CH_3$ and $–CH_2$ groups into HA with CTA^+ cations results in the intensity increase in the two bands [33]. The stretching band of –OH groups at 3450 cm^{-1} did not change after the complexing reaction, indicating that –OH groups of HA were not involved in the reaction.

High-resolution N1s XPS spectra of HA and HA–CTA are shown in Figs. 3(a) and (b). Only one N1s XPS peak is seen at 399.8 eV for native HA, associated with the only N

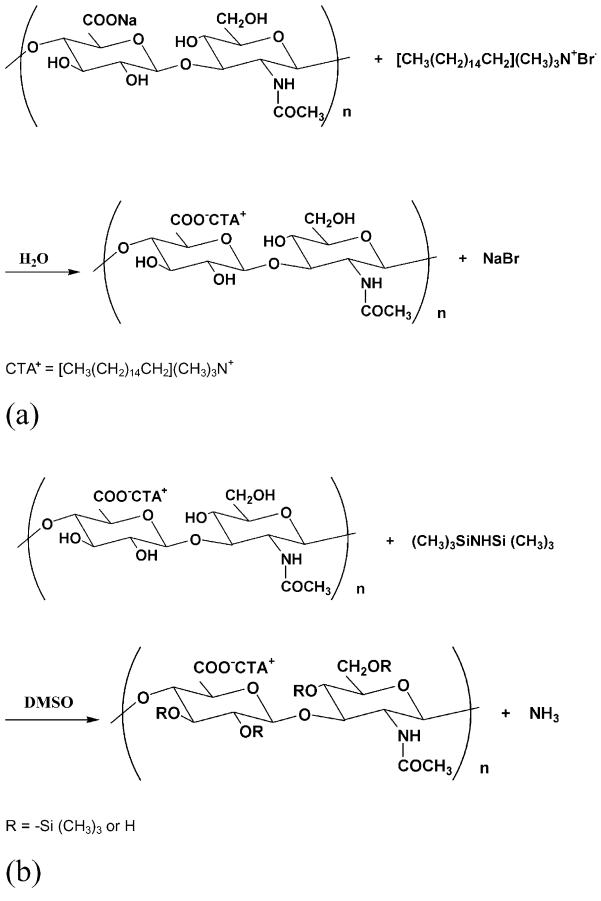

Fig. 1. Reactions: (a) precipitation of HA with CTAB; (b) silylation of HA–CTA.

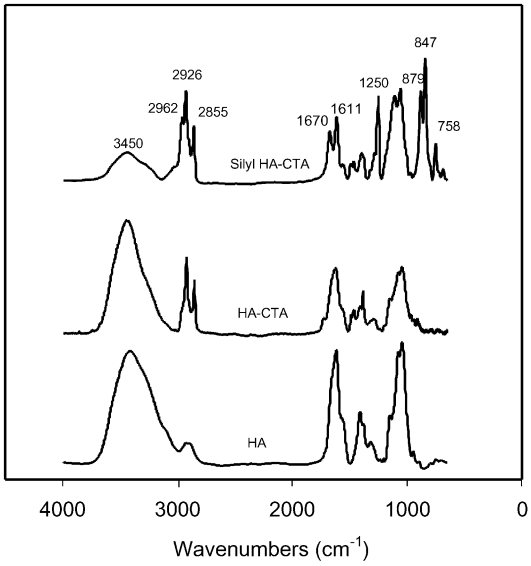

Fig. 2. FT-IR spectra of HA, HA–CTA and silyl HA–CTA.

atom present in the amide group (–CO*N*H–) of HA [34]. The N1s spectrum of HA–CTA can be best fit with two peaks (one at 399.8 eV, another at 402.8 eV) because the quaternary ammonium nitrogen (CTA ammonium salt N^+, also represented as N^+Q) leads to the new peak at 402.8 eV [34]. The intensity of the two peak components should theoretically be the same, due to the 1:1 molar ratio between $–COO^-N^+Q$ and –CONH– in HA–CTA. This is confirmed by N1s XPS analysis below for silyl HA–CTA. However, in Fig. 3(b) the peak at 402.8 eV has a greater intensity than the peak at 399.8 eV due to CTAB residue present in the HA–CTA product.

The ^{1}H NMR spectrum for HA–CTA (Fig. 4(b)) shows completely different characteristics from that of HA (Fig. 4(a)). In the ^{1}H NMR spectrum of HA, the strongest resonance centered at 4.80 ppm is due to residual H_2O present in D_2O and the water absorbed by HA. Several other small peaks around 4.80 ppm correspond to the anomeric protons (2H) and the hydroxyl protons (4H) [35–37]. The broad signals at 3–4 ppm are assigned to the non-anomeric protons (10H) [38]. The three methyl protons of C*H*$_3$-CONH– are represented by a peak centered at 1.95 ppm. In the ^{1}H NMR spectrum of HA–CTA, several new peaks appear with disappearance of the HA resonances around 4.80 and 1.95 ppm, and the shape and position of the signals at 3–4 ppm are also changed. The new triplet at 0.851 ppm is attributed to the methyl protons in the cetyl groups ($–CH_2(CH_2)_{14}CH_3$) of CTA, while the strong peak at 1.236 ppm is due to the methylene protons in cetyl groups ($–CH_2(CH_2)_{14}CH_3$), and the intensity ratio of these two peaks is 3.1:26.54, very close to the theoretical value of 3:28. The broad resonance at 1.650 ppm could be assigned to the protons of the methyl or methylene groups connected to the quaternary N^+ cation ($–CTA^+$). The multiplet centered at 2.50 ppm comprises the DMSO-d_6 solvent

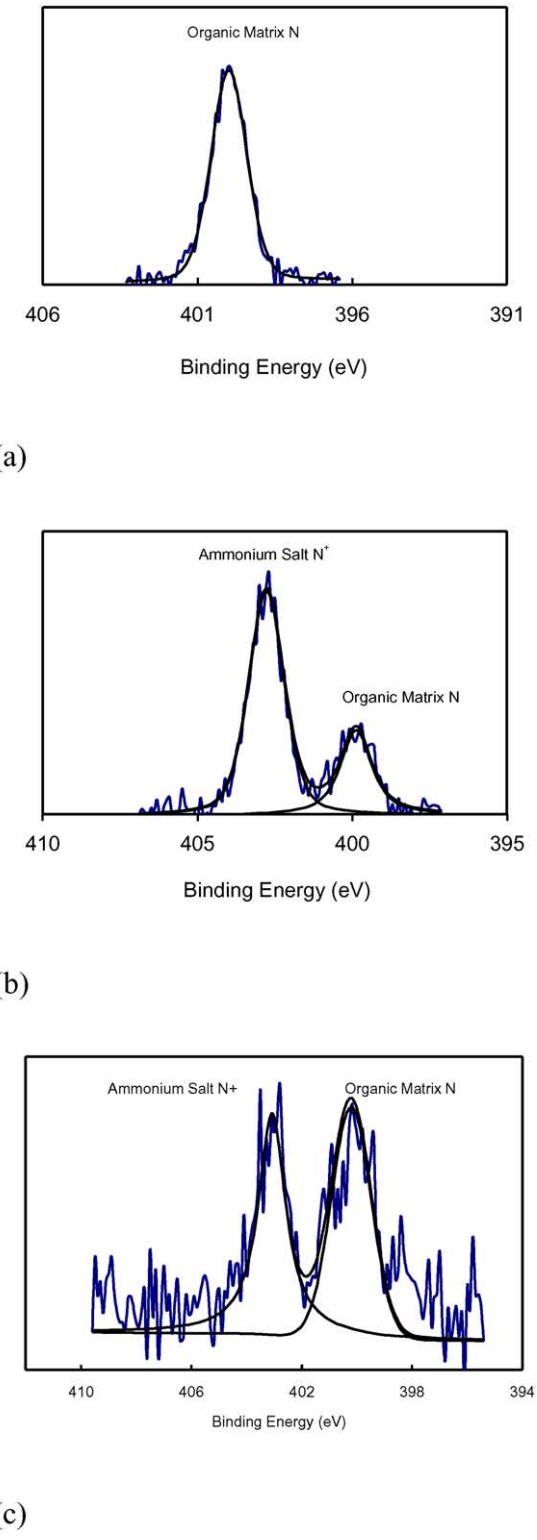

Fig. 3. High-resolution XPS N1s spectra of (a) HA; (b) HA–CTA; (c) silyl HA–CTA.

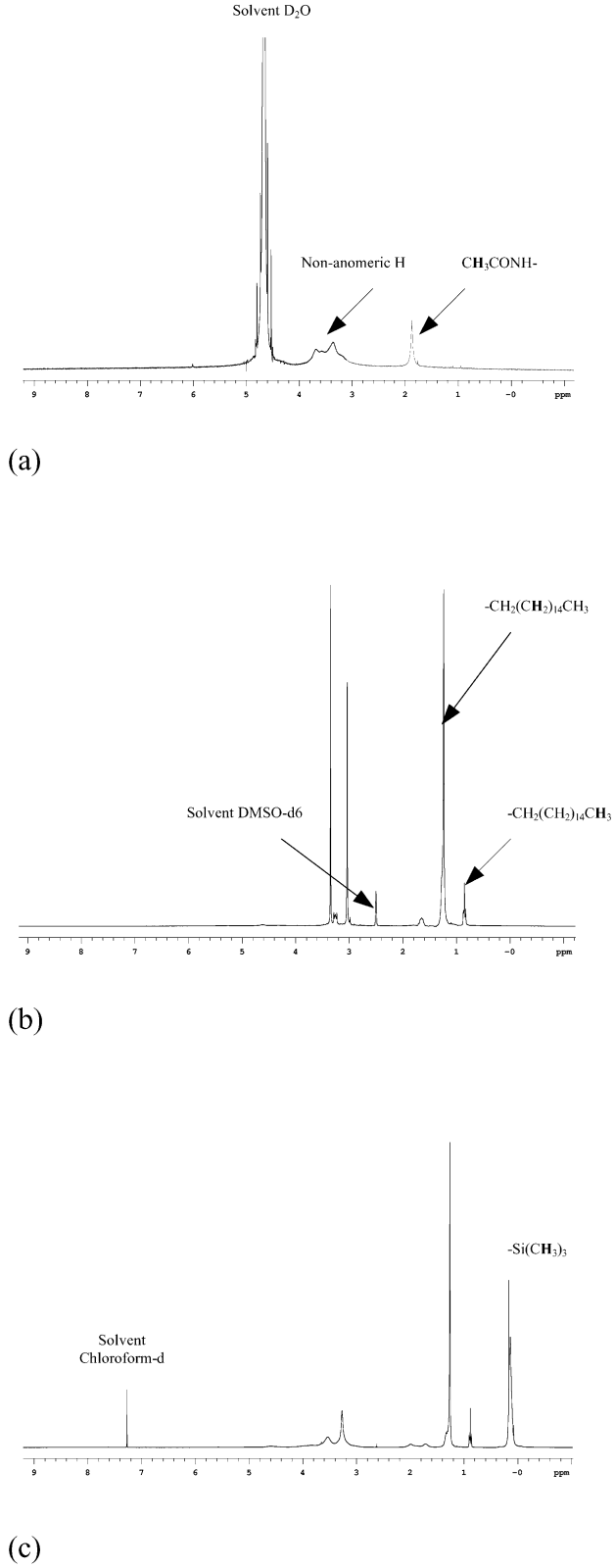

Fig. 4. ^{1}H NMR spectra of (a) HA; (b) HA–CTA; (c) silyl HA–CTA.

peaks. The number of protons introduced with CTA is large compared to that in each HA disaccharide unit, so some peaks for the HA protons are too weak to be visible in the HA–CTA spectrum. Due to interaction with solvents, the same protons, especially in –OH and –NH_x groups, may show different resonances in different solvents [37]. This might be the reason for the change of signals at 3–4 ppm.

The ^{13}C NMR spectrum of HA–CTA is shown in Fig. 5(a). The strong multiplet centered at 40.207 ppm is due to the solvent DMSO-d_6. Peaks at 14.664, 22.801, 29.757, 31.989, and 52.809 ppm, respectively, represent the different carbons of –CTA (C1, C2, C4, C3 and C5) [37]. A desirable ^{13}C NMR spectrum of HA was not obtained in this study due to the difficulty of making higher concentrations of HA, but it can be found elsewhere [35,39]. The reported carbon resonances for HA are not observed in ^{13}C NMR spectrum of HA–CTA. This may be because these signals are too weak to be seen.

HA can only be dissolved in water, but HA–CTA is soluble in highly polar solvents (e.g. DMSO and formamide). Thus, HA–CTA can be used for the starting material of non-aqueous reactions, such as silylation. HA–CTA was found to be an effective starting material for the silylation reaction after many attempts to directly silylate HA failed. Varied combinations of silylating agents (e.g. TMCS, BSA and HMDS) and solvents (e.g. THF, DMSO, DMF and pyridine) based on the silylation methods used for cellulose, chitin and dextran were also unsuccessfully applied to HA. HA is very hygroscopic. The water HA absorbs from air may interfere with silylation of the HA because water is a more reactive silyl acceptor. Toluene was used to boil HA and remove water via forming an azeotrope. Even after dehydration, HA still did not react with silylation agents. Therefore, the strong inter- and intra-molecular interactions (hydrogen bonds) and lack of solubility in silylation solvent were hypothesized to be the main reason that –OH groups on HA resist attack from silylation agents. Similar phenomena make silylation of cellulose very sluggish [22]. The long aliphatic chains in quaternary ammonium cations ($-CTA^+$) were effective in disrupting the hydrogen bonds and increasing the solubility of HA in silylation solvents.

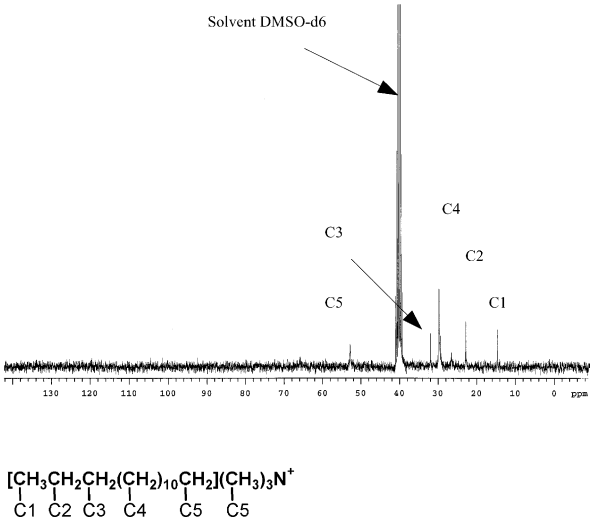

Fig. 5. ^{13}C NMR spectra of (a) HA–CTA; (b) silyl HA–CTA.

3.2. Silylation of HA–CTA

In silylation, the –OH groups of HA–CTA were substituted by $-OSi(CH_3)_3$ groups (Fig. 1(b)). FT-IR spectra shown in Fig. 2 confirm the structural changes. The silyl HA–CTA spectrum shows four new pronounced peaks, characteristic of the absorption of $-OSi(CH_3)_3$ groups. The intense band at 1250 cm^{-1} is associated with symmetric bending of $Si–CH_3$ [33]. The two strong peaks at 847 and 758 cm^{-1} are assigned to rocking of $Si(CH_3)_3$. Another strong absorption at 879 cm^{-1} corresponds to vibration of Si–OC [40]. The appearance of a small peak at 2962 cm^{-1} represents the introduced $–CH_3$ groups from the trimethylsilyl residue. It is also noticed that the stretching band of –OH and amide –NH– moities (around 3450 cm^{-1}) in silyl HA–CTA is very weak compared with that in HA–CTA and native HA, due to the replacement of most –OH by $-OSi(CH_3)_3$. Two separate carbonyl –C=O stretch bands are seen at 1670 and 1611 cm^{-1} in silyl HA–CTA: one attributable to amide I (–C=O in the secondary amide –NHC=O) [41], another due to carboxylate $-COO^-$ [33]. The two vibrations overlap in HA and HA–CTA near 1620 cm^{-1}. In silyl HA–CTA, the inter- and intra-molecular interaction is completely disrupted by the introduction of $-Si(CH_3)_3$, resulting in a hydrogen-bond free environment and causing the shift of the amide I band to a much higher frequency (1670 cm^{-1}). The IR vibration frequency of amide I is sensitive to its environment, such as hydrogen bonding. The stronger the hydrogen bond, the lower the frequency of the amide I absorption [41].

Like HA–CTA, the N1s XPS spectrum of silyl HA–CTA (Fig. 3(c)) can also be split into two peaks: ammonium salt N^+ component and amide N component. Their peak areas are almost identical, indicating that the silylation reaction did not involve or alter the CTA groups complexed with HA carboxyl groups, but did remove the CTAB residue that had resulted in unequal peak intensities in Fig. 3(b).

In the ^1H NMR spectrum of silyl HA–CTA (Fig. 4(c)), the typical resonance of trimethylsilyl protons ($-Si(CH_3)_3$) is observed at 0.162 ppm [37]. Another new peak at

7.270 ppm is due to residual chloroform present in the chloroform-d. The two resonances at 0.851 and 1.236 ppm, present in the ^{1}H NMR spectrum of HA–CTA and attributed to the methyl and methylene protons in the cetyl groups, still exist in the ^{1}H NMR spectrum of silyl HA–CTA. Furthermore, the intensity ratio of these two resonances did not change (3.31:27.91), confirming that the –CTA groups were not involved in silylation. The intensity ratio of the trimethylsilyl proton peak at 0.162 ppm and the methylene proton peak at 1.236 ppm is 36:27.91, almost equal to 36:28, indicating four –Si(CH_3)$_3$ groups for each –CTA group ($CH_3(CH_2)_{14}CH_2(CH_3)_3N^+$). Thus, all four –OH groups of this HA–CTA sample silylated at 75 °C for 24 h have been replaced by –Si(CH_3)$_3$.

In comparison to the ^{13}C NMR spectrum of HA–CTA, two new peaks appear in ^{13}C NMR spectrum of silyl HA–CTA (Fig. 5(b)). The triplet centered at 77.23 ppm represents the solvent chloroform-d. The signal around 0 ppm indicates the presence of –Si(CH_3)$_3$ [37,42].

Although HA could not be silylated, the complex HA–CTA soluble in DMSO (a good silylation solvent) reacted with typical silylation agents, such as BSA, TMCS and HMDS. Based on the criteria of high or moderate reactivity and easy separation of product, HMDS was selected for the silylation agent. TMCS and BSA are more active than HMDS. However, removal of excess BSA and its by-products are difficult due to their high boiling temperature (BSA: 71–73 °C/35 mm Hg; acetamide: 221 °C). The higher-chlorinated silane impurities in TMCS, dimethyldichlorosilane ($(CH_3)_2SiCl_2$) and methyltrichlorosilane ($(CH_3)SiCl_3$), easily caused crosslinking of the silylated polymer. The low boiling point (125 °C), gas by-product (NH_3) and easily separated products made HMDS a good choice of silyation agent in this study. HMDS is not soluble in DMSO. It forms a separate phase floating on DMSO. HA–CTA dissolved in DMSO reacts with HMDS at the interface. Vigorous stirring is therefore very important to keep the two phases interspersed sufficiently to assure completion of the reaction.

3.3. The effect of silylation conditions on DS

The effect of silylation temperature and time on the degree of silylation (DS) was investigated and the results are shown in Table 1 and Fig. 6. Theoretically, the only primary hydroxyl group in HA should be more reactive than other three secondary hydroxyl groups. However, it is noticed that the DS values are always larger than 1 even at low temperature or at insufficient silylation reagent conditions, indicating the good reactivity of the three secondary –OH groups. Furthermore, since the trimethylsilyl group is not bulky, the differences in reactivity of the three secondary –OH groups caused by steric effects is not significant.

For the same sample, the DS values from the different calculation methods vary. Compared with the DS from weight gain, the DS from FT-IR is smaller, while that from Si content is larger. However, they all exhibit the same trends with reaction conditions. In Fig. 6, it is found that a nearly complete silylation can be achieved at 75 °C within 24 h. This result is in agreement with the DS = 4 obtained from the ^{1}H NMR analysis. However, at least 72 h are required to reach the same DS for silylation at 55 °C. The reactions at both temperatures are fast before DS = 3, but after that they proceed slowly, especially when close to DS = 4.

Table 1
The effect of reaction temperature and time on DS

Silylation (temp× time)	DS from weight gain	DS from FTIR	Si content (%)	DS from %Si
55 °C×12 h	2.58	2.13	10.64	3.46
55 °C×24 h	3.18	2.88	–	–
55 °C×48 h	3.48	2.93	–	–
55 °C×72 h	3.75	3.12	12.38	4.29
75 °C×12 h	2.97	2.81	11.93	4.07
75 °C×24 h	3.80	3.00	–	–
75 °C×36 h	3.84	3.25	–	–
75 °C×48 h	3.96	3.39	12.95	4.59

The HMDS /OH molar ratio for all reactions was 10:1.

It is necessary to discuss the relationship between the three DS calculation methods to find a convenient and accurate method to control the reaction. Because the silylated products were subject to a vacuum until reaching a constant weight, the DS calculated from weight gain should be accurate and thus were used to plot Fig. 6. The FT-IR method can be easily used to test the DS during reaction. However, the DS values calculated from FT-IR are below that obtained with the weight gain method, due to the conflicting presence of the amide –NH vibration at 3500 cm^{-1}. The DS values from FT-IR need to be calibrated with those from weight gain [18]. A linear correlation between the two DS values is obtained (Fig. 7). With this calibration, the simpler FT-IR method can be used to determine the DS with very little product during silylation. The DS values calculated from Si content are much higher than those from both FT-IR and weight gain methods. The high DS may come from inaccuracies in the Si content measurement, and/or be due to Si contamination of

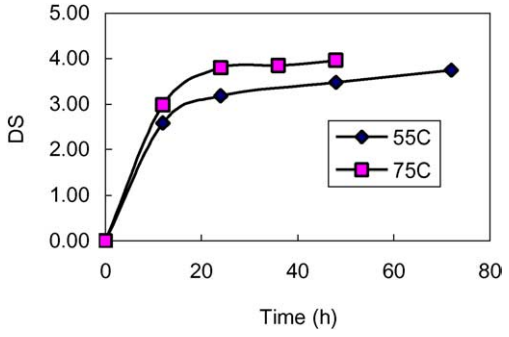

Fig. 6. The effect of silylation temperature and time on the DS from weight gain.

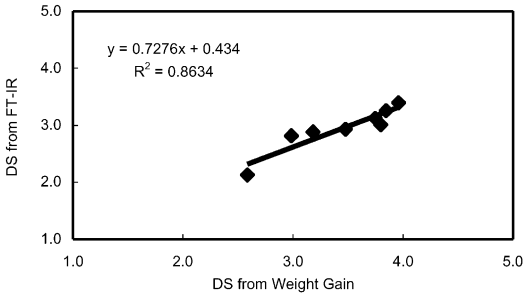

Fig. 7. Relationship between the DS from FT-IR and the DS from weight gain.

the samples from the laboratory (e.g. vacuum grease used in silylation equipment). Small amounts of Si contamination would significantly skew the DS values from the Si content method because the DS from that method is proportional to the content of all Si in the sample.

The molar ratio of HMDS/–OH also affected the degree of silylation (Table 2). An increase in the ratio enhanced the silylation, but beyond a ratio of 5:1, the increase leveled off. To continue increasing the DS, a higher temperature may be required.

The above discussion provides evidence that the degree of the silylation can be controlled through adjusting the reaction temperature and time, and the HMDS/–OH molar ratio. By doing this, silyl products with different solubility in organic solvents can be obtained to meet various solubility requirements. The silyl HA–CTA with DS (from weight gain method) larger than 3.2 can be dissolved in hexane and xylenes, while those with DS smaller than 3.2 but larger than 2.5 are soluble in acetone, THF and 1,2-dichloroethane. This enables processing HA with more hydrophobic polymers and facilitating further derivatization reactions.

3.4. Thermal degradation of HA

The properties of HA and its derivatives highly depend on HA molecular weight. Whether the high silylation temperatures caused degradation of the HA–CTA molecular chains was a concern. Intrinsic viscosity is the most common measure for polymer molecular weight (M_w); the relationship between the two parameters is governed by the Mark–Houwink–Sakurada equation. Because of the lack of K and α values for HA–CTA in DMSO solution, HA in aqueous solution was utilized to examine the effect of temperature and time on the degradation of HA. Under the same conditions, the degradation of HA in water should be greater that that of HA–CTA in DMSO due to the potential for hydrolysis in the presence of water.

Table 2
The effect of HMDS/OH ratio on DS

HMDS/OH molar ratio	DS from FTIR[a]
1:1	1.67
5:1	2.62
10:1	2.88
30:1	2.92

[a] All silylation was carried out at 55 °C for 24 h.

HA aqueous degradation results are shown in Table 3. Tests were only performed at 55 and 75 °C because all silylation temperatures were within that range. The molecular weight loss at 55 °C up to 87 h is less than 11.5%, and the loss at 75 °C up to 48 h less than 10.5%. Because the practical silylation was carried out in an anhydrous environment for a much shorter time, the degradation of HA–CTA molecular weight during silylation should be very small.

A strange phenomenon is also found in examining these degradation data. The molecular weight of HA seems to significantly increase first and then decline at both test temperatures. This is in agreement with what Lowry and Beavers [29] observed when examining the effect of temperature on the viscosity of HA. They explained the phenomenon with the viscoelastic behavior of HA. The viscosity of HA at a temperature above 25 °C depends on the balance of two opposite factors. One is thermally induced polymer chain scission, and another is the increased molecular volume caused by further separation of chain segments at a higher temperature, which enhances the entanglement of HA molecules and leads to an increase in viscosity [30]. At the beginning of degradation, the latter factor dominates, causing an increased viscosity. However, as degradation continues, the latter is overtaken by the former, exhibiting typical degradation characteristics.

3.5. Regeneration of HA

To restore the hydrophilic, lubricious and other desirable properties of HA, it is necessary to regenerate HA from its derivatives. The FT-IR spectra for the HA regenerated from HA–CTA and silyl HA–CTA are shown in Fig. 8. All vibrational peaks associated with $–Si(CH_3)_3$ and –CTA vibrations are gone. These two spectra are the same as that for original HA, indicating the success in removing –CTA from HA–CTA and both $–Si(CH_3)_3$ and –CTA from silyl HA–CTA through hydrolysis. For use of HA as a biomaterial, there may be toxicity concerns with residual

Table 3
Intrinsic viscosity and molecular weight of HA after thermal degradation

Degradation condition	Intrinsic viscosity (l/g)	M_w ($\times 10^6$ Da)	ΔM_w (%)
Non-degradation	1.8511	1.0388	0
55 °C×16 h	1.9350	1.0968	5.6
55 °C×48 h	1.7859	0.9942	−4.3
55 °C×87 h	1.6757	0.9195	−11.5
75 °C×16 h	1.9053	1.0762	3.6
75 °C×30 h	1.6901	0.9292	−10.5
75 °C×48 h	1.7535	0.9721	−6.4

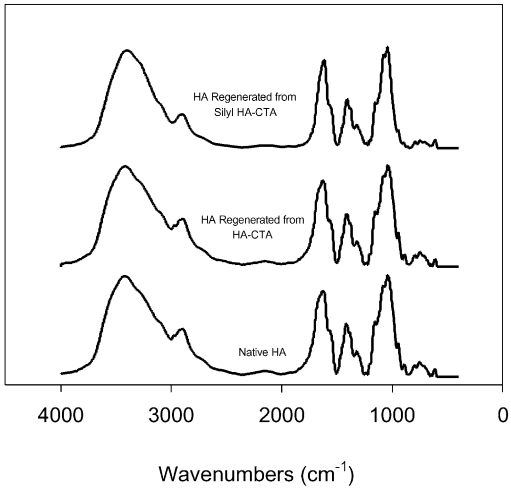

Fig. 8. FT-IR spectra of HA regenerated from HA–CTA and silyl HA–CTA, and native HA.

Si. However, since the boiling point of hexamethyldisiloxane is 101 °C any residue, which is not rinsed off during HA precipitation with ethanol, can be easily removed through vacuum drying.

3.6. Properties of HA and silyl HA–CTA

HA–CTA is a white bulk material. It must be cut into small pieces before use in silylation reaction. The polymer is soluble in DMSO and formamide, yielding a transparent viscous solution. It also dissolves in concentrated NaCl solution (≥ 0.2 M) via ion exchange. However, it is insoluble in acetone, ethanol, xylenes, pyridine, hexane, and other less polar solvents. The film cast from HA–CTA in DMSO solution was clear and flexible. Sharp creasing did not break it. It appears that the thermal stability of HA–CTA is inferior to that of its parent polymer HA ($T_d \sim 212$ °C) (Fig. 9). This may be attributed to disruption of polymer hydrogen bonds and the crystalline regions by the long –CTA side chain, which enhances access of oxygen to the polymer chains in the crystalline regions.

Silyl HA–CTA is a colorless to slightly yellow powder depending on the degree of silylation. When the DS is low ($2.5 < DS \leq 3.2$), the colorless silyl HA–CTA is insoluble in xylenes, but soluble in THF, acetone, and 1,2-dicholoroethane. The solution-cast film is clear and also flexible. The silyl HA–CTA with $DS > 3.2$ is light yellow, and soluble in xylenes and hexane. Its film cast from xylenes solution is clear, but brittle.

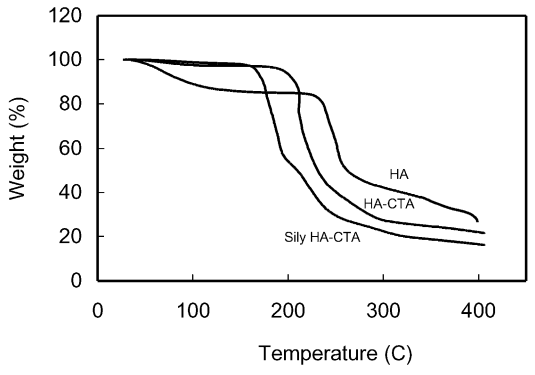

Fig. 9. TGA thermograms of HA, HA–CTA and silyl HA–CTA.

Silyl HA–CTA is stable in air. Polymer samples left in ambient air for one year were still completely soluble in xylenes. At room temperature, silyl HA–CTA did not dissolve in water, but did swell after several days. When the water was heated to 40–50 °C, the silyl HA–CTA particles were hydrolyzed and then dissolved within several days. Silylation further decreased the thermal stability of HA. The decomposition of silyl HA–CTA starts (around 161 °C) at much lower temperatures than HA and HA–CTA. The low cleavage energy of Si–C bonds in the O–Si$(CH_3)_3$ groups attached to HA–CTA molecules and the further disruption of crystalline regions in HA–CTA (and thus, enhanced oxidation) may explain this.

4. Conclusions

The HA complex with aliphatic ammonium salts was soluble in highly polar organic solvents, and thus can be used as a reaction intermediate. HA was successfully silylated with HA–CTA as the starting material. Silylated HA was soluble in acetone, THF, 1,2-dichloroethane, xylenes and hexane, depending the silylation degree (DS). The degree of silylation could be controlled through modulation of the reaction temperature and time, and the silylation agent/–OH ratio.

HMDS was demonstrated to be an effective silylating agent, due to its easily separated product and gas by-product. The minimal degradation of HA molecules under silylation conditions was acceptable, because even in water solution the decrease in HA molecular weight was less than 12%.

Through silylation reaction, HA became hydrophobic, soluble in non-polar organic solvents, and compatible with other hydrophobic biomaterials. Furthermore, the modified groups can be easily removed through hydrolysis to regenerate native HA. Finally, the silylated HA derivatives are more reactive than native HA, making them useful as the intermediate for further modifications of HA.

Acknowledgements

Thanks to Dr David Grainger for his invaluable advice and assistance, to Dr Guy Beauregard for his training on silylation technique.

References

[1] Laurent TC. In: Balazs EA, editor. Chemistry and molecular biology of the intercellular matrix, vol. 2. London: Academic Press; 1970. p. 703–28.
[2] Balazs EA, Gibbs DA. In: Balazs EA, editor. Chemistry and molecular biology of the intercellular matrix, vol. 3. London: Academic Press; 1970. p. 1241–53.
[3] Balazs EA, Band P. Cosmetics Toiletries 1984;99:65–72.
[4] Hoekstra D. Med Device Diagn Ind 1999;51–8.
[5] Ogston AG. In: Balazs EA, editor. Chemistry and molecular biology of the intercellular matrix, vol. 3. London: Academic Press; 1970. p. 1231–9.
[6] Heinegard D, Björnsson S, Mörgelin M, Sommarin Y. In: Laurent TC, editor. The chemistry, biology and medical applications of hyaluronan and its derivatives. London: Portland Press Ltd; 1998. p. 113–21.
[7] Weiss C. In: Abatangelo G, Weigel PH, editors. New frontiers in medical science: redefining hyaluronan. Amsterdam: Elsevier; 2000. p. 89–100.
[8] Balazs EA, Denlinger JL. The biology of hyaluronan. In: Evered D, Whelan J, editors. Ciba foundation symposium 143. Chichester: Wiley; 1989. p. 265–73.
[9] Weiss C. In: Laurent TC, editor. The chemistry, biology and medical applications of hyaluronan and its derivatives. London: Portland Press Ltd; 1998. p. 255–65.
[10] Biomatrix, Inc.. In: Kennedy JF, Phillips GO, Williams PA, Hascall VC, editors. Hyaluronan 2000, vol. 2. Cambridge: Woodhead Publishing Limited; 2002. p. 3–5 [see also p. 461–465].
[11] Yun YH, Goetz DJ, Yellen P, Chen W. Biomaterials 2004;25:147–57.
[12] Grigolo B, Roseti L, Fiorini M, et al. Biomaterials 2001;22:2417–24.
[13] Brun P, Cortivo R, Radice M, Abatangelo G. In: Abatangelo G, Weigel PH, editors. New frontiers in medical science: redefining hyaluronan. Amsterdam: Elsevier; 2000. p. 269–78.
[14] Defife KM, Shive MS, Hagen KM, et al. J Biomed Mater Res 1999; 44:298–307.
[15] Balazs EA, Larsen NE. In: Garg HG, Longaker MT, editors. Scareless wound healing. New York: Marcel Dekker; 2000. p. 143–60.
[16] Harmon RE, De KK, Gupta SK. Carbohydr Res 1973;31:407–9.
[17] Pierce AE. Silylation of organic compounds. Rockford: Pierce Chemical Company; 1968 [p. 1–26].
[18] Mormann W, Demeter J, Wagner T. Macromol Chem Phys 1999;200: 693–7.
[19] Cooper GK, Sandberg KR, Hinck JF. J Appl Polym Sci 1981;26: 3828–35.
[20] Hermanutz F, Gähr F, Pirngadi P, et al. Chem Fibers Int 2001;51: 271–2.
[21] Schuyten HA, Weaver JW, Reid JD, Jurgens JF. J Am Chem Soc 1948;70:1919–20.
[22] Harmon RE, De KK. Cellulose technology research. In: Turbak AF, editor. ACS symposium series 10. Washington, DC: American Chemical Society; 1975. p. 39–50.
[23] Kurita K. Prog Polym Sci 2001;26:1921–71.
[24] Ydens I, Rutot D, Degée P, et al. Macromolecules 2000;33:6713–21.
[25] Scott JE. Chem Ind 1955;168–9.
[26] Scott JE. Methods Biochem Anal 1960;8:145–97.
[27] Goussé C, Chanzy H, Excoffier G, Soubeyrand L, Fleury E. Polymer 2002;43:2645–51.
[28] Haxaire K, Maréchal Y, Milas M, Rinaudo M. Biopolymers 2003;72: 10–20.
[29] Lowry KM, Beavers EM. J Biomed Mater Res 1994;28:1239–44.
[30] Gura E, Hückel M, Müller PJ. Polym Degrad Stab 1998;59:297–302.
[31] Laurent TC, Ryan M, Pietruszkiewicz A. Biochim Biophys Acta 1960;42:476–85.
[32] Rodriguez F. Principles of polymer systems. 4th ed. Washington, DC: Taylor and Francis; 1996 [p. 225–289].
[33] Smith B. Infrared spectral interpretation. New York: CRC Press; 1998 [p. 158–160].
[34] Moulder JF, Stickle WF, Sobol PE, Bomben KD. Handbook of X-ray photoelectron spectroscopy. Eden Prairie (MN): Physical Electronics Division; 1992.
[35] Crescenzi V, Francescangeli A, Taglienti A, et al. Biomacromolecules 2003;4:1045–54.
[36] Nouvel C, Ydens I, Degée P, et al. Polymer 2002;43:1735–43.
[37] Günther H. NMR spectroscopy. 2nd ed. Chichester (England): Wiley; 1994.
[38] Crescenzi V, Francescangeli A, Renier D, Bellini D. Macromolecules 2001;34:6367–72.
[39] Cowman MK, Hittner DM, Feder-Davis J. Macromolecules 1996;29: 2894–902.
[40] Zollfrank C. Wood Sci Technol 2001;35:183–9.
[41] Griebenow K, Santos AM, Carrasquillo KG. Internet J Vib Spectro 1999;3. 1st ed http://www.ijvs.com/volume3/edition1/section3a.htm.
[42] Monsef-Mirzai P, Manak H, McWhinnie WR, et al. Fuel 1998;77: 369–74.